Clinical Study

Ear, Nose & Throat Journal
2021, Vol. 100(1) NP57–NP61

DOI: 10.1177/0145561319862786
journals.sagepub.com/home/ear
SAGE

Evaluation of the Golden Ratio in Nasal Conchae for Surgical Anatomy

Emine Petekkaya, PhD[1], Mahinur Ulusoy, MD[1], Hassan Bagheri, MSc[1], Şükrü Şanlı, MD[2], Mehmet Seyit Ceylan, MD[3], Mehmet Dokur, MD[4], and Mehmet Karadağ, PhD[5]

Abstract

Purpose: The golden ratio is reached by the fractal model of the number sequence which is known as the "Fibonacci series" and has a convergent ratio of approximately 1.618 between 2 consecutive Fibonacci numbers. Golden ratio relationships have been shown in several plants in the nature and several organs and structures in the human body. The conchae, which form an important part of the nasal valve, have a special geometric significant in terms of providing turbulence to the laminar airflow that passes to the nasal cavity. **Methods:** This study made golden ratio calculations on 34 adults aged 20 to 45 years over computed tomography (CT) images. Totally, 34 volunteers (male, n = 18 and female, n = 16) with no nasal pathologies participated in the study. Using Adobe Photoshop, golden ratio calculations were made by applying the Fibonacci spiral on the images that best showed the conchae and meatuses on the CT images. **Results:** The intersection points of the spiral that was projected on the inferior and middle nasal concha were determined as S0, S1, S2, S3, and S4. The distances of S0-S1, S1-S2, S2-S3, and S3-S4 were measured. The concha measurements of the women showed significantly similar values to the golden ratio constant of ~1.618 in the RS3/S4 and LS3/S4 measurements. **Conclusion:** We found that the S3/S4 region that captured the golden ratio in our study corresponds to the base part of the inferior nasal concha, and its place of spiraling in the nasal cavity is observed to have an important role in creating vortices.

Keywords

ınferior nasal concha, Fibonacci spiral, measurements, golden ratio, surgical anatomy

Introduction

The golden ratio or divine proportion is a mathematical ratio that is also known to be represented by the Greek letter phi (ϕ) and obtained by converging to the numerical value of approximately 1.618. It is known that high levels of visual aesthetics are provided by some geometric shapes with the golden ratio, for example, a rectangle with the golden ratio between its height and width. Such a rectangle may be divided into a square or another golden rectangle based on the order of the Fibonacci series. The golden ratio has become a center of attention not only for noticeable aesthetical pleasure in the fields of art, architecture, and music but also because of its connection to the structures and functions of the human body. Golden ratio relationships have been demonstrated in several plants in nature and several organs and structures in the human body.[1,2] The presence of proportional aesthetics has been associated with heart valves and coronary branching,[3] emergence of the aorta from the left ventricle,[4] ratios of bodily lengths to each other,[5] face modeling,[6] bronchial branching,[7] and childhood costal development.[8] The spiral-like scrolled structure of the inferior nasal concha led us to determine whether or not this region also has the golden ratio. Human nasal cavity is an important component that serves various physiological functions. In addition to filtering pollutant substances and poisonous particles that may enter the airways from the incoming air, it is also responsible for warming and humidifying the breathed air for the body temperature to be matched.[9] The lateral wall of

[1] Department of Anatomy, The Faculty of Medicine, Campus of Beylikdüzü, University of Beykent, Büyükçekmece-Istanbul, Turkey
[2] Department of Radiology, The Faculty of Medicine, University of Biruni, Florya-Istanbul, Turkey
[3] Department of Otolaryngology, The Faculty of Medicine, Sani Konukoğlu Hospital Practice and Research Center, University of Sanko, Şehitkamil-Gaziantep, Turkey
[4] Department of Emergency Medicine, The Faculty of Medicine, University of Biruni, Florya-Istanbul, Turkey
[5] Department of Biostatistics, The Faculty of Medicine, University of Istanbul Okan, Tuzla-Istanbul, Turkey

Received: June 5, 2019; revised: July 16, 2019; accepted: July 19, 2019

Corresponding Author:
Emine Petekkaya, PhD, Department of Anatomy, The Faculty of Medicine, University of Beykent, Campus of Büyükçekmece , 34520, Büyükçekmece-Istanbul, Turkey.
Email: eminepetekkaya@beykent.edu.tr

the nasal cavity contains 3 projections of variable size called the superior, medius, and inferior nasal conchae, which are 3 spongy bone laminae. Their functions are protecting the entrance of the sinuses and increasing surface area. Conchae are thin bones covered with ciliated respiratory mucosa. These structures divide the airway into 3 passages and create paths that are called meatus under the conchae. While the right and left sides of the human nasal cavity geometrically differ, there are also interpersonal nasal morphological differences. It was reported that about half of the airflow that passes through the nasal cavity passes through the inferior and middle nasal meatus, while a small part of the air passes through the olfactory area. Presence of a "golden ratio" in both the flow velocity of air and the anatomical dimensions of the cavity was found by calculating the cross-sectional area ratio between the anterior and posterior parts of the nasal cavity as $44/26 = 1.69$.[9]

Our study aimed to investigate the bone structures belonging to that passage that creates turbulence and vortices on the laminar airflow through this particular geometrical structure of the nasal cavity in relation to the golden ratio and the effects of this ratio.

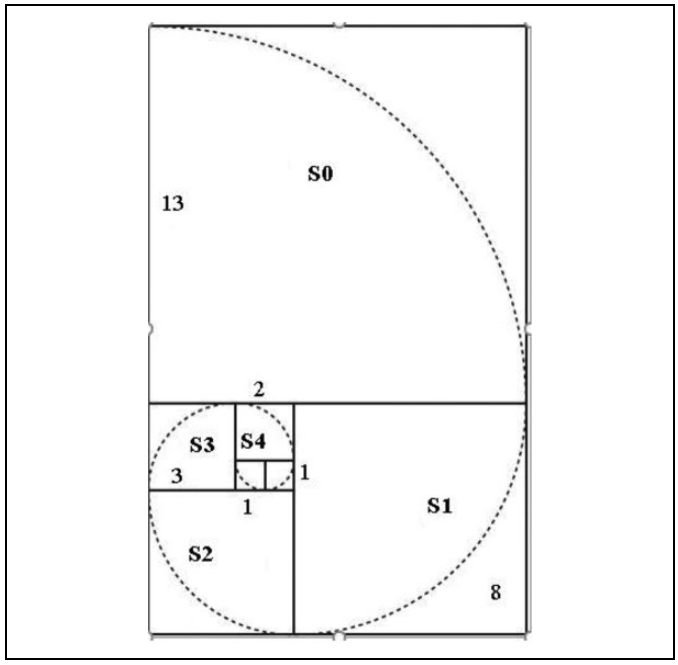

Figure 1. Golden rectangle and golden spiral.

Material and Methods

Ethic Statement

The experimental protocol was approved by the local institutional animal ethics review committee (Ethical permission no: 2018/23-07, Biruni University Ethical Committee). All experiments were conducted in compliance with the relevant laws and institutional guidelines.

Data Collection and Processing

The study included 34 adult volunteers without no nasal pathologies (male, n = 18 and female, n = 16). The paranasal computed tomography (CT) images with coronal plans of the adult individuals aged 20 to 45 years were included. The study continued with individuals with no nasal pathology or septum deviation. Individuals with allergic rhinitis, vasomotor rhinitis, deviated septum, or concha hypertrophy were excluded from the study. In all cases, same first sections including 3 conchae and meatuses were selected from among the coronal CT images and processes using the Adobe Photoshop software. Then a rectangle was projected lengthwise on each nasal cavity passage. The superior nasal concha, where the aeration is minimal, was left outside the rectangle. After the Fibonacci spiral was completely placed over the middle nasal concha and inferior nasal concha, some points that were compatible with the circular ratios of the spiral were determined. The base part of the inferior nasal concha that extends freely in the nasal cavity formed the starting point of the spiral.

Measuring Technique for Golden Ratio

Golden ratio calculations using Adobe Photoshop were made by applying the Fibonacci spiral. The precise value of golden ratio may also be expressed on a line partitioned into 2 unequal lengths (shorter length [S] and longer length [L] in such a manner that $L/S = (L + S)/L =$ Golden Ratio (≈ 1.618).[10] The intersection points of the spiral that was projected on the inferior and middle nasal concha were determined as S0, S1, S2, S3, and S4. When the diagonal lines of all rectangles are connected by an arc, the last quarter circle converges to the golden spiral. These points were determined in a way to show the intersection points of the spiral with the golden square and rectangle that corresponded to the spiral's consecutive numbers of 0-1-2 as S4 (first rectangle), 3 as S3 (second rectangle), 5 as S2 (third rectangle), 8 as S1 (fourth rectangle), and 13 as S0 (fifth rectangle; Figure 1). The S0-S1, S1-S2, S2-S3, and S3-S4 distances were measured (Figures 2 and 3).

Statistical Analysis

In order to determine whether or not these values differed significantly from the golden ratio, the analysis of the characteristics that were normally distributed was carried out in one group by one-sample *t* test, while the non-normally distributed measurements were analyzed by Wilcoxon signed-rank test, and *P* values less than .05 were considered statistically significant. SPSS version 16.0 for Windows was used for the statistical analyses.

Results

The CT images of 18 male and 16 female participants were used in the study. The mean age was 40.72 ± 13.51 years for the men and 42.69 ± 15.04 years for the women. According to the results of the one-sample *t* test that was conducted to determine whether or not the measurements of the men differed significantly from 1.618, the mean value of the measurements was significantly different ($P > .05$). According to the results of

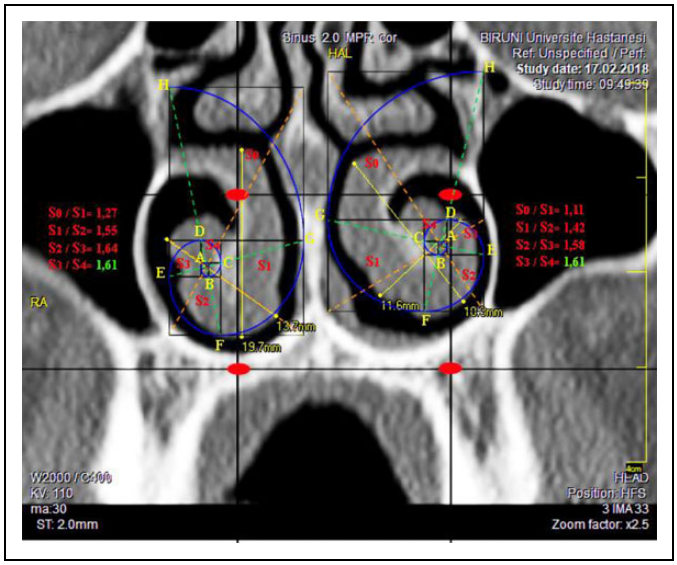

Figure 2. Calculation of the golden ratios of the conchae with the Fibonacci spiral (male).

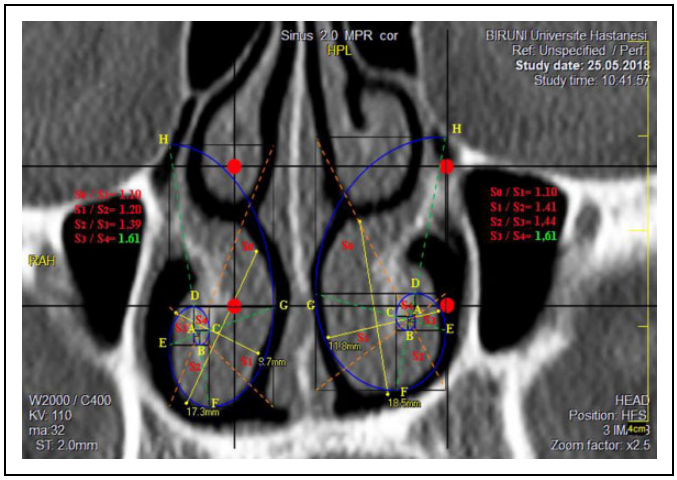

Figure 3. Calculation of the golden ratios of the conchae with the Fibonacci spiral (female).

the one-sample *t* test that was conducted to determine whether or not the measurements of the women differed significantly from approximately 1.618, the RS3/S4 and LS3/S4 measurements were significantly similar ($P < .05$). In the results that provided differences based on sex, the incidence of the women for approaching the golden ratio at the base of the inferior nasal concha (the points S4-S3) was found to be higher in comparison to the men (Table 1).

Table 1. Golden Ratio Analysis of Men and Women.

	Male (n = 18)	Female (n = 16)		
Variables	Mean ± Standard Deviation	Mean ± Standard Deviation	Test Statistics	*P*
AGE	40.72 ± 13.51	42.69 ± 15.04	$t = -0.401$	.691
RS0	7.69 ± 2.31	9.06 ± 1.49	$z = -2.073$	.038[a]
RS1	6.44 ± 1.82	7.51 ± 1.34	$t = -1.940$	.061
RS2	4.73 ± 1.08	4.91 ± 0.84	$t = -0.550$	.586
RS3	3.37 ± 1.33	3.18 ± 0.54	$z = -0.086$	.931
RS4	1.94 ± 0.5	1.97 ± 0.33	$t = -0.164$	.871
RS0/S1	1.12 ± 0.23	1.22 ± 0.13	$t = 1.464$	.154
RS1/S2	1.43 ± 0.14	1.51 ± 0.07	$t = -2.112$	.045[a]
RS2/S3	1.48 ± 0.12	1.55 ± 0.09	$t = -1.693$	.100
RS3/S4	1.64 ± 0.03	1.61 ± 0.05	$z = -1.896$	.058
LS0	7.96 ± 2.3	9.15 ± 1.36	$t = -1.856$	.074
LS1	6.69 ± 1.49	7.52 ± 1.37	$t = -1.679$	.103
LS2	4.64 ± 1.06	5.07 ± 0.86	$t = -1.288$	.207
LS3	3.11 ± 0.95	3.26 ± 0.58	$z = -0.017$	.986
LS4	1.97 ± 0.4	2.02 ± 0.35	$t = -0.359$	.722
LS0/S1	1.19 ± 0.28	1.23 ± 0.15	$t = -0.481$	.633
LS1/S2	1.44 ± 0.12	1.47 ± 0.13	$t = -0.621$	0.539
LS2/S3	1.43 ± 0.16	1.57 ± 0.06	$t = -3.472$	.002[a]
LS3/S4	1.65 ± 0.03	1.61 ± 0.05	$z = -2.341$	.019[a]
R-LENGTH	9.8 ± 1.96	10.81 ± 1.95	$t = -1.507$	.142
R-WIDTH	16.85 ± 2.57	15.67 ± 2.54	$t = 1.344$	.188
L-LENGTH	9.47 ± 1.89	11 ± 1.83	$t = -2.388$	.023[a]
L-WIDTH	17.43 ± 2.38	15.93 ± 3.36	$t = 1.518$	.139

[a]$P < .05$, *t*, Student *t* test, z, Mann-Whitney *U* test.

Discussion

The common theme of all calculations adapted to all biological systems using Fibonacci spiral is to obtain the universal constant or golden ratio ($\phi = 1.61803$).[11-13] Our study which investigated the presence of the golden ratio in the nasal conchae observed that the conchae followed a logarithmic spiral shape. Observation of the presence of the golden ratio especially in the turbulence and vortex formation areas of the concha structures during nasal airflow showed that the aerodynamic effect may be influential on determining the centers of turbulence formation. The geometric and mucosal structure of the nasal cavity is significant in serving important function such as cleaning, warming, and humidifying air. The extension of the nasal conchae toward the nasal cavity creates a laminar flow effect on the airflow.[14] When the air that is breathed in passes through the nasal valve region, the laminar airflow turns into a turbulence that extends the contact time between the inspiratory air and the surrounding mucosa. The kinetic energy of the turbulent airflow allows contact of the inspiratory air and the mucosa. A vortex forms in the area where turbulence is achieved.[14] It is expected that these functions are related to the complicated inner geometry of the nose. Especially the middle and inferior nasal conchae are important structures that increase the surface area of the mucosal wall for filtration, warming, and humidification. While the inferior nasal concha is described as the place where the velocity of airflow is the highest, the middle nasal concha has been shown as the place where aeration is the highest.[9] Nasal airway obstructions due to concha hypertrophy or cartilaginous factors lead to respiratory problems. Respiratory functions which have vital significance take place in an area that needs surgical operation the most frequently due to disrupted nasal geometry.

Nevertheless, satisfaction rates after surgery are still low. It is important to be able to determine the connection between airflow patterns and the geometry of the nose for improving these situations. The inferior concha is composed of the bony shell, the submucosal tissue, and the overlying mucosa. Surgical procedures involve resecting, ablating, or crushing part, or all, of the turbinate to increase the size of the nasal airway. The appropriate choice of procedure may depend on a patient's anatomy and other concurrent procedures performed (such as septoplasty or septorhinoplasty) as well as the presence or absence of other comorbidities such as allergic rhinitis. The golden ratio may be helpful in deciding which surgical method (crushing, bony resection, submucosal ablation) to choose for the lower turbinate. Examinations of nasal geometry are possible by 2-dimensional imaging methods.[15,16] For 3-dimensional examinations, airflow dynamics may be analyzed by creating nasal models.[9] In this study, the CT nasal structure examination for 34 adults was achieved by a 2-dimensional method. There were sex-related differences in our study, and the incidence of approaching the golden ratio was higher in the women. The S3/S4 region of the right and left nasal valves that is shown as the region that achieved the golden ratio corresponds to the base of the inferior nasal concha, and the role of the place where it scrolls in the nasal cavity in creating vortices seems important. The studies by Wen et al[9] and Croce et al[17] reported that 2 vortices are formed in the nasal cavity, while the large one is formed in the inferior nasal concha region for respiration functions and the small one is formed in the olfactory region for the sense of smell.

Our study included a 2-dimensional evaluation of the relationship between the composition of bone structures and golden ratio in healthy adult individuals. Obviously, this is far from reflecting the dynamic changes of the mucosa and submucosal tissue covering the nose. However, most surgical procedures such as septoplasty, septorhinoplasty, turbinoplasty, and nasal valve surgery for the nose nasal are intended to alter the composition of the bone and cartilage structure. Moreover, these procedures aim to expand the nasal valve region in 2 dimensions.[18,19] Therefore, golden ratio can provide us with a useful perspective to evaluate the pathological anatomical status of the nose. The golden ratios of individuals with normal nasal anatomy and normal nasal functions have been evaluated in this study. The extent to which these values change in pathological conditions and their reflections to the clinic need more studies. Investigation of the correlation between acoustic rhinomanometry and peak nasal inspiratory flowmetry methods can reveal the relationship of the golden ratio with nasal functions.

Limitations

Although our study was limited to cross-sectional examination of bone structures, it may provide ideas for future studies where the mucosal effect will also be investigated. Comparisons may be carried out between this golden ratio and individuals with airflow disorders to contribute to clinical practice. It is recommended to examine the concha structures of individuals in different age groups for determining age-related differences.

Conclusion

The concha measurements of the women showed significantly similar values to the golden ratio constant of $\sim$1.618 in the RS3/S4 and LS3/S4 measurements. The S3/S4 region that is shown in our study as the region that achieved the golden ratio corresponds to the base of the inferior nasal concha, and the role of the place where it scrolls in the nasal cavity in creating vortices seems important. We believe that a disruption of the ratio that we obtained at the base of the inferior nasal concha may cause various clinical situations by disrupting the turbulent characteristics of the air that is taken into the nasal cavity.

Authors' Note

Oral presentation at 19th National Anatomy Congress and International Mediterranean Anatomy Congress, September 6-9, 2018, Konya, Turkey. The study was performed in accordance with the 2011 Guide for the Care and Use of Laboratory Animals.

Declaration of Conflicting Interests

The author(s) declared no potential conflicts of interest with respect to the research, authorship, and/or publication of this article.

Funding

The author(s) received no financial support for the research, authorship, and/or publication of this article.

ORCID iD

Emine Petekkaya https://orcid.org/0000-0002-5366-2425

References

1. Akhtaruzzaman M, Shafie AA. Geometrical substantiation of Phi, the golden ratio and the baroque of nature, architecture, design and engineering. *Int J Art*. 2011;1(1):1-22. doi:10.5923/j.arts.20110101.01.
2. Persaud-Sharma D, O'Leary JP. Fibonacci series, golden proportions, and the human biology. *Austin J Surg*. 2015;2(5):1066.
3. Ashrafian H, Athanasiou T. Fibonacci series and coronary anatomy. *Heart Lung and Circ*. 2011;20(7):483-484. doi:10.1016/j.hlc.2011.02.008.
4. Aparci M, Celik T, Yalcin M, Isilak Z. Golden ratio between left ventricular and aortic dimensions. *Int J Cardiol*. 2016;205:60-61. doi:10.1016/j.ijcard.2015.
5. Davis TA, Altevogt R. Golden mean of the human body, Fibonacci Q. 1979;17:344-384.
6. Schwind V. *The Golden Ratio in 3D Human Face Modeling*. Stuttgart, Germany: Stuttgart Media University; 2011. https://vali.de/?p=1117. Accessed April 23, 2019.

7. Goldberger AL, West BJ, Dresselhaus T, Bhargava V. Bronchial asymmetry and Fibonacci scaling. *Experientia*. 1985;41(12): 1537-1538.
8. Schwend RM, Schmidt JA, Reigrut JL, Blakemore LC, Akbarnia BA. Patterns of rib growth in the human. *Child. Spine Deformity*. 2015;3(4):297-302. doi:10.1016/j.jspd.2015.01.007.
9. Wen J, Inthavong K, Tu J, Wang S. Numerical simulations for detailed airflow dynamics in a human nasal cavity. *Respir Physiol Neurobiol*. 2008;161(2):125-135. doi:10.1016/j.resp.2008.01.012.
10. Yalta K, Ozturk S, Yetkin E. Golden ratio and the heart: a review of divine aesthetics. *Int J Cardiol*. 2016;214:107-112. doi:10.1016/j.ijcard.2016.03.166.
11. Akhtaruzzaman M, Shafie AA. https://shininglotus.com/newsletters/2016-newsletters/2016-december-newsletter/golden-section-ratio-divine-proportion-and-golden-spiral/. Accessed April 23, 2019.
12. Liu Y, Sumpter DJT. Is the golden ratio a universal constant for self-replication? *PLoS One*. 2018;13(7):e0200601. https://doi.org/10.1371/journal.pone.0200601.eCollection2018.
13. Condello I, Nasso G, Fiore F, et al. Fibonacci's golden ratio—an innovative approach to the design and management of extra-corporeal circulation. *Surg Technol Int*. 2019;34:340-350. pii: sti34/1104.
14. Sevinc O, Barut C, Kacar D, Is M. Evaluation of the lateral wall of the nasal cavity in relation to septal deviation. *Int J Morphol*. 2013;31(2):438-443.
15. Kelly JT, Prasad AK, Wexler AS. Detailed flow patterns in the nasal cavity. *J. Appl. Physiol*. 2000;89(1):323-337. doi:10.1152/jappl.2000.89.1.323.
16. Churchill SE, Shackelford LL, Georgi JN, Black MT. Morphological variation and airflow dynamics in the human nose. *Am J Hum Biol*. 2004;16(6):625-638. doi:10.1002/ajhb.20074.
17. Croce C, Fodil R, Durand M, et al. In vitro experiments and numerical simulations of airflow in realistic nasal airway geometry. *Ann Biomed Eng*. 2006;34(6):997-1007. doi:10.1007/s10439-006-9094-8.
18. Cantone E, Ricciardiello F, Oliva F, De Corso E, Iengo M. Septoplasty: is it possible to identify potential "predictors" of surgical success?. *Acta Otorhinolaryngol Ital*. 2018;38(6):528-535. doi:10.14639/0392-100X-2072.
19. Zojaji R, Keshavarzmanesh M, Bakhshaee M, Behdani R, Esmaeelzadeh S, Mazloum FarsiBaf M. The effects of inferior turbinoplasty on nasal airflow during cosmetic rhinoplasty. *Acta Otorhinolaryngol Ital*. 2016;36(2):97-100. doi:10.14639/0392-100X-410.